

## Solitonlike Propagation of Exciton-Polariton Pulses Supported by Biexciton Two-Photon Dispersion

Kazuhiro Ema\* and Makoto Kuwata-Gonokami

*Department of Applied Physics, Faculty of Engineering, The University of Tokyo, 7-3-1 Hongo, Bunkyo-ku, Tokyo 113, Japan*  
(Received 30 November 1994; revised manuscript received 8 March 1995)

We present a new scheme of distortion free propagation of exciton-polariton pulses in the low-intensity region. In this scheme, the anomalous nonlinear dispersion associated with the biexciton two-photon transition compensates the group velocity dispersion to maintain the pulse duration. We demonstrate the distortion free propagation of polariton pulses in CuCl. We compare the observed pulse profiles with the calculated profiles using the frequency domain wave equation, where the lowest-order coherent nonlinearity is taken into account. We obtain good agreement between the experiment and the calculation.

PACS numbers: 42.50.Md, 42.50.Rh, 71.35.+z

Nonlinear propagation of an ultrafast optical pulse is of interest for its application to high bit rate optical communication and ultrafast optical devices. In particular, the formation of solitons in optical fibers has been studied extensively. In these studies, the carrier frequency of the optical pulse is set to be far off resonant from the absorption edge of the material, and the quadratic group velocity dispersion (GVD), the lowest-order dispersion term, is compensated by the third-order nonlinearity expressed with the nonlinear refractive index  $n_2$  which is a real number with no frequency dependence. The temporal and spatial evolution of optical pulses in such a situation can be analyzed with the nonlinear Schrödinger equation (NSE). In the actual system, the higher-order dispersion terms or finite response time of the material affect the stability of optical solitons. Although some extreme cases such as shock term [1] have been examined in the frame of NSE, the effect of nonlinear dispersion on the pulse propagation characteristics has not been fully explored. On the other hand, distortion free optical pulse propagation in the resonant region is also an issue of current interest because of their importance in the ultrafast optical switching devices such as the semiconductor directional coupler. In the resonant region, however, NSE is not a good approach, because  $n_2$  shows a strong frequency dependence, and higher-order nonlinear terms are important. Several types of polariton solitons at exciton resonance have been proposed [2–7]. An experiment is conducted in a semiconductor waveguide structure [8]. In these studies, the pulse duration is maintained by the higher-order light-matter interaction, that is a strong contrast to the case of NSE where only the lowest-order coherent nonlinear interaction is included.

In this paper, we propose a new scheme of solitonlike propagation, where a strong GVD is compensated by a nonlinear anomalous dispersion. A typical example of the nonlinear anomalous dispersion is a two-photon resonance (TPR) dispersion [9]. The TPR anomalous dispersion could compensate a strong linear dispersion of one-photon resonance shown in Fig. 1. We now consider a

three-level system and pulse propagation at the TPR of the highest level  $c$ . The level  $b$  is allowed for a dipole transition from the ground level, and the dipole transition causes a polariton dispersion. Figure 1(b) schematically shows that the TPR anomalous dispersion compensates the polariton GVD at the TPR. Thus we can expect a solitonlike propagation under a certain condition. The optical nonlinearity at the half band gap region in a semiconductor has potentiality for this scheme. However, incoherent process prevails and obscures the resonant coherent effect [10,11]. Biexciton TPR is another candidate for this scheme. There exist very large coherent optical nonlinearities at the biexciton TPR because of the giant dipole moment [12–17]. We explain this scheme using a frequency domain wave equation considering the lowest-order coherent nonlinearity. We demonstrate the scheme presenting the femtosecond polariton pulse propagation at the biexciton TPR in CuCl. The results are compared with numerical calculations.

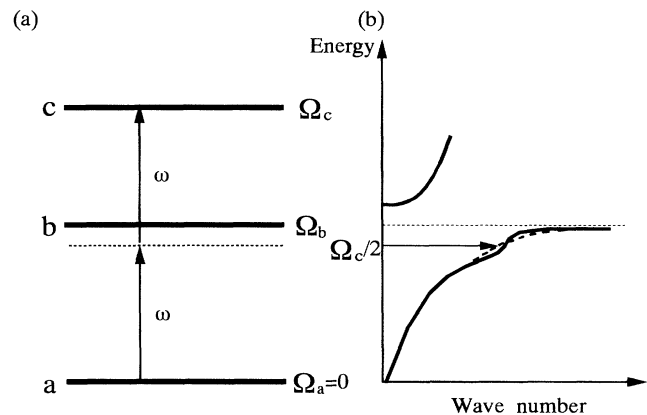


FIG. 1. Schematic illustration of an energy diagram of a three-level system (a) and a dispersion curve (b). A pulse propagates at a two-photon resonance of level  $c$ . The solid and dotted dispersion curves represent the polariton dispersion with and without nonlinear dispersion, respectively. The anomalous dispersion of the two-photon resonance compensates a strong linear dispersion.

Fourier components of the electric field of the pulse in the form of running wave is

$$E(\omega, z) \equiv \hat{E}(\omega, z)e^{ik(\omega)z}, \quad k^2(\omega) = \frac{\omega^2}{c^2} [1 + \chi^{(1)}(\omega)], \quad (1)$$

where  $k(\omega)$  is the complex wave number and  $\hat{E}(\omega, z)$  is the complex envelope function. Within a slowly varying envelope approximation, the derivative of  $\hat{E}(\omega, z)$  with respect to  $z$  is expressed as [18]

$$\begin{aligned} \frac{\partial}{\partial z} \hat{E}(\omega, z) &= i \frac{1}{2k(\omega)} \left( \frac{\omega}{c} \right)^2 \\ &\times \int d\omega_1 \int d\omega_2 \chi^{(3)}(\omega : \omega_1, \omega_2, \omega_1 + \omega_2 - \omega) \hat{E}(\omega_1, z) \hat{E}(\omega_2, z) \hat{E}^*(\omega_1 + \omega_2 - \omega, z) e^{i\Delta kz}, \end{aligned} \quad (2)$$

where we take account of only the lowest nonlinearity  $\chi^{(3)}$  because we consider sufficiently low intense pulses, and  $\Delta k$  represents phase mismatch

$$\Delta k = k(\omega_1) + k(\omega_2) - k^*(\omega_1 + \omega_2 - \omega) - k(\omega). \quad (3)$$

We consider a propagation at the TPR region shown in Fig. 1. If the energy difference  $\Delta\Omega = \Omega_b - \Omega_c/2$  is much larger than the spectral width of  $\hat{E}(\omega, z)$ ,  $\chi^{(3)}$  is dominated by the TPR terms. In CuCl, the binding energy of  $\Gamma_1$  biexciton is about 30 meV, which is larger than the spectral width of the subpicosecond input pulse. Thus we can provisionally use  $\chi^{(3)}$  for the subpicosecond pulse propagation at biexciton TPR in CuCl,

$$\begin{aligned} \chi^{(3)}(\omega; \omega_1, \omega_2, \omega - \omega_1 - \omega_2) &= \frac{N\mu_e^2\mu_m^2}{\Omega_m - \omega_1 - \omega_2 - i\gamma_m} \frac{1}{\Omega_T - \omega - i\gamma} \\ &\times \left( \frac{1}{\Omega_T - \omega_1 - i\gamma} + \frac{1}{\Omega_T - \omega_2 - i\gamma} \right) + \chi_{\text{nr}}^{(3)}, \end{aligned} \quad (4)$$

where  $N$  is the number of unit cells per unit volume,  $\mu_e$  is a transition dipole moment of the exciton,  $\mu_m$  is the giant dipole moment of the transition between the biexciton and the exciton,  $\Omega_m$  and  $\Omega_T$  are the resonance frequencies of the biexciton and the transverse exciton, and  $\gamma_m$  and  $\gamma$  are the dephasing constants of the biexciton and the exciton [19]. The nonresonant term  $\chi_{\text{nr}}^{(3)}$  of Eq. (4)

includes exciton resonance terms [ $\propto N\mu_e^4/(\omega - \Omega_T)^3$ ], which are much smaller than the biexciton term because of the large detuning. We ignore the term in the following discussion.

As the first approximation, we neglect the phase-mismatched terms in Eq. (2) by putting  $\omega_2 = \omega$  in the integral,

$$\frac{\partial}{\partial z} \hat{E}(\omega, z) = i \frac{1}{2k(\omega)} \left( \frac{\omega}{c} \right)^2 \int \chi^{(3)}(\omega : \omega_1, \omega, -\omega_1) |\hat{E}(\omega_1, z)|^2 e^{-2k_i(\omega_1)z} d\omega_1 \hat{E}(\omega, z), \quad (5)$$

where  $k_i(\omega)$  is the imaginary part of the linear wave number  $k(\omega)$ . If the attenuation of the pulse is negligible [i.e., both  $k_i(\omega)$  and  $\text{Im}\chi^{(3)}$  are small], we can replace  $|\hat{E}(\omega_1, z)|^2 e^{-2k_i(\omega_1)z}$  in the integrand of Eq. (5) by  $|\hat{E}(\omega_1, 0)|^2$ . In this case, the solution of Eq. (5) has the following form:

$$\hat{E}(\omega, z) = \hat{E}(\omega, 0) e^{ik^{\text{NL}}(\omega)z}, \quad (6)$$

where nonlinear change in the wave vector  $k^{\text{NL}}(\omega)$  is defined as

$$k^{\text{NL}}(\omega) = \frac{1}{2k(\omega)} \left( \frac{\omega}{c} \right)^2 \int \chi^{(3)}(\omega : \omega_1, \omega, -\omega_1) |\hat{E}(\omega_1, 0)|^2 d\omega_1, \quad (7)$$

which has anomalous dispersion in the vicinity of biexciton TPR frequency. In Fig. 2, the solid curve shows the dispersion curve of the real part with nonlinear dispersion [ $k(\omega) + k^{\text{NL}}(\omega)$ ] and the dotted curve shows the linear dispersion curve [ $k(\omega)$ ].  $k(\omega)$  can be derived from the exciton-polariton dispersion equation. In the numerical calculation, we use material parameters of the bulk CuCl:  $\Omega_T = 3.202$  eV,  $\Omega_L = 3.2079$  eV,  $\Omega_m = 6.3722$  eV,  $\gamma = 0.03$  meV,  $\gamma_m = 0.5$  meV,  $\varepsilon_B = 5.59$ ,  $M = 2.3m_0$ ,  $N = (4/5.41)^3 \text{ \AA}^{-3}$ ,  $\mu_e = 0.083 e \text{ \AA}$ , and

$\mu_m = 7 e \text{ \AA}$ . We set the input pulse with width 300 fs (FWHM) and center frequency 3.186 eV (biexciton TPR resonance frequency). As we can see in Fig. 2, the nonlinear dispersion compensates polariton dispersion in the frequency region of the input pulse at a certain intensity. In this curve, the compensated region is about 3 meV which is much larger than the biexciton linewidth,  $\gamma_m$ . This is because  $k^{\text{NL}}(\omega)$  is produced by the integration over the whole spectral region of the input pulse. We use the value of  $\gamma_m = 0.5$  meV in the calculation to get

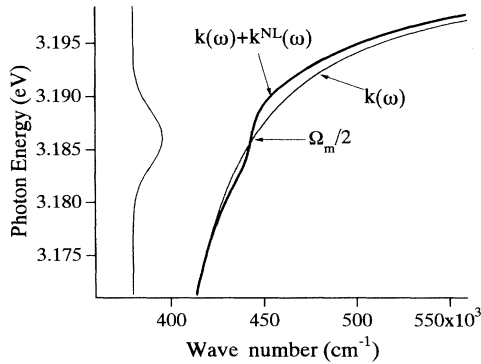


FIG. 2. The real part of the linear polariton dispersion  $k(\omega)$  (dotted curve) and the total dispersion with the nonlinear dispersion  $k(\omega) + k^{\text{NL}}(\omega)$  (solid curve) for the input pulse whose duration is 300 fs, the frequency is 3.186 eV (equal to biexciton TPR). The nonlinear dispersion  $k^{\text{NL}}(\omega)$  compensate polariton dispersion for the frequency region of the input pulse. The input-pulse spectrum  $\hat{E}(\omega, 0)$  is illustrated in the left side of the figure.

clear compensation for the spectral region which corresponds to the 300 fs pulse. The dephasing constant of  $\gamma_m$  of 0.5 meV is much larger than the known value which is measured by the frequency domain [20] and time domain [21–23] methods under the weak excitation condition. Such a large value, however, is consistent with the value obtained from the analysis of nonlinear change in the polariton dispersion measured with hyper Raman scattering [16,17,24].

In the actual system, we have to take into account the attenuation of the pulse. We calculate changes of the pulse shape along  $z$  using Eq. (2), including phase-mismatched terms and linear and nonlinear attenuation effects. Figure 3(a) shows the results of the numerical calculation of the pulse shape transmitted through the 10  $\mu\text{m}$  sample. The sample is discretized into 600 slices. The dotted curves show the intensity profiles of the output pulses calculated using Eq. (2), whereas the solid curves are the profiles calculated using the nonlinear dispersion. When the input pulse intensity is weak enough, the pulse duration increases because of the strong group velocity dispersion of polaritons near the exciton resonance. By increasing the pulse intensity, the pulse duration becomes shorter and the group velocity increases. Solid curves clearly show distortion free propagation, while small distortions remain in the dotted curves. These distortions are caused by the nonlinear absorption and the non-phase-matched terms.

We use a high purity single crystal of CuCl with a thickness of 10  $\mu\text{m}$  and keep them at 10 K. Frequency-doubled mode-locked Ti:Al<sub>2</sub>O<sub>3</sub> laser (pulse width is 300 fs) is tuned to the biexciton TPR (3.186 eV). The biexciton state has  $\Gamma_1$  symmetry and has no angular momentum. Thus the biexciton two-photon transition is al-

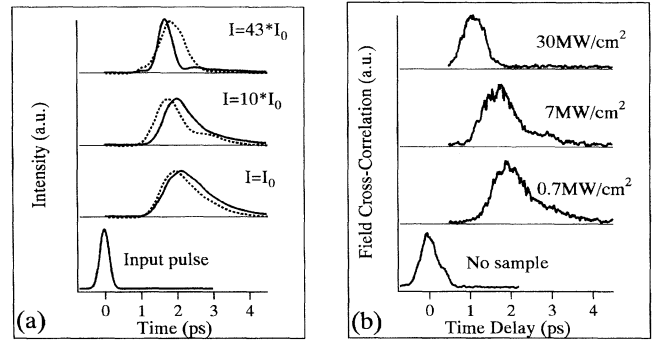


FIG. 3. (a) The calculated pulse shapes. The solid curve represents the intensity profile derived by using the nonlinear dispersion  $k^{\text{NL}}(\omega)$ . The dotted curve is derived using Eq. (2). In these calculations we use material parameters of CuCl. (b) The measured amplitude of field-cross correlations of the transmitted linear-polarized pulses. The thickness of the sample is 10  $\mu\text{m}$ . The pulse width and frequency of the input pulse are 300 fs and 3.186 eV. The time delay zero point is the time when the pulse peaks without the sample.

lowed for a single linearly polarized beam but forbidden for a single circularly polarized beam. We perform the experiments with a circularly polarized beam and a linearly polarized beam to clarify the biexciton TPR effect. Shapes of the transmitted pulses are measured by the field cross-correlation technique. We superimpose the transmitted pulse beam on a reference pulse beam and measure the amplitude of interference fringes as a function of delay time of the reference pulse beam. A part of the input pulse beam is used as the reference pulse beam. The amplitude of the fringes coincides with the pulse shape, as long as the phase variation of the output pulse is less than  $\pi$  within the duration of the reference pulse. The numerical calculations show that the maximum phase variation of the transmitted pulses is approximately 1.5 rad, so we use this technique to determine pulse shapes. Figure 3(b) shows the experimental results for linearly polarized pulses. We observe strong distortion by GVD at weak intensity. The observed pulse shape agrees with the calculated curve. With increasing the intensity, we clearly see the narrowing of the pulse duration and the increase in the velocity. For circularly polarized pulses, no pulse narrowing is observed.

We should show that the pulse intensity in our experiment is in the low excitation region where the lowest-order nonlinearity is dominant. In the renormalized dielectric function [25,26] which contains the higher nonlinear effects, the expression of the susceptibility has a whole set of odd order of  $|\mu_m E|^2 / \gamma_m (\Omega_T - \Omega_m/2)$  at the biexciton TPR ( $\omega = \Omega_m/2$ ). If the experimental condition satisfies the inequality

$$\frac{|\mu_m E|^2}{\gamma_m (\Omega_T - \Omega_m/2)} \ll 1, \quad (8)$$

we can reduce the nonlinear change in the dielectric function into the lowest-order term  $\chi^{(3)}$ . The maximum peak intensity (30 MW/cm<sup>2</sup>) is corresponding to the field amplitude  $|E|^2 \approx 1.8 \times 10^{12}$  (V/m)<sup>2</sup>, which satisfies the condition of Eq. (8). We also estimate the biexciton density by the amount of two-photon absorption. The density is less than  $10^{15}$  cm<sup>-3</sup>, thus we can safely ignore the higher-order processes such as biexciton-polariton scatterings and biexciton-biexciton collisions. When the excitation pulse duration is longer than biexciton lifetime (50 to 100 ps), the accumulation of excitons occurs and the higher-order effects become important. We use subpicosecond pulses, so we can ignore the accumulation effects in our pulse energy region.

As we can see in Fig. 3, the experimental results agree with the curves calculated with the nonlinear dispersion  $k^{\text{NL}}(\omega)$  of Eq. (7). This implies that the attenuation of the pulse and effects of phase-mismatched terms are very small in our experiments. Actually the ratio between the intensity of the input and the output pulse is approximately 0.7 including reflection loss. The ratio has little dependence on the intensity. We suppose that the effective  $\gamma_m$  relevant to the real part of  $\chi^{(3)}$  (which affects the dispersion curve) is larger than the effective  $\gamma_m$  for the imaginary part (which causes two-photon absorptions). Similar discrepancy between the real and imaginary parts of  $\chi^{(3)}$  has been seen in the experimental results on nonlinear ellipsometry [27]. The large values of  $\gamma_m$  ranging from 0.2 to 0.4 meV are used to explain the experimental data of the nonlinear shift of the hyper Raman scattering lines. Nonlocality in the nonlinear optical response caused by the finite translational mass of biexcitons causes such discrepancy.

The increase in the group velocity is also caused by a modification of exciton-polariton dispersion associated with the exciton resonant terms. As we can see in Fig. 2 the high energy part of the dispersion curve is sensitive to the exciton resonant terms, which lead to the reduction of GVD. The observed increase in the group velocity is larger than that of the calculation. We actually observe a slight increase in the group velocity even for circularly polarized pulses. Thus the nonresonant term,  $\chi_{\text{nr}}^{(3)}$ , which we neglect in the calculation, reduces the group velocity.

In summary, we present a new scheme of distortion free propagation of exciton polariton, and demonstrate it experimentally in CuCl.

This work was supported by the Grant-in-Aid for Priority Area Grant No. 06245208 by the Ministry of Education, Science, and Culture of Japan.

---

\*Present address: Department of Physics, Sophia University, 7-1 Kioicyo, Chiyoda-ku, Tokyo 102, Japan.

- [1] A. Hasegawa, *Optical Solitons in Fibers* (Springer-Verlag, Berlin, 1989); G.P. Agrawal, *Nonlinear Fiber Optics* (Academic Press, Boston, 1989), Chap. 2.
- [2] A. Knorr, R. Bibder, M. Lindberg, and S. W. Koch, *Phys. Rev. A* **46**, 7179 (1992).
- [3] A.D. Boardman, G.C. Cooper, A.A. Maradudin, and T.P. Shen, *Phys. Rev. B* **34**, 8273 (1986).
- [4] A.L. Ivanov and V.V. Panashchenko, *Sov. Phys. JETP* **72**, 882 (1991).
- [5] A.L. Ivanov and G.S. Vygovskii, *Solid State Commun.* **78**, 787 (1991).
- [6] K.T. Stoychev and M.T. Primatarowa, *Phys. Rev. B* **46**, 10727 (1992).
- [7] I.B. Talanina, M.A. Collins, and V.M. Agranovich, *Solid State Commun.* **88**, 541 (1993).
- [8] P.A. Harten, A. Knorr, J.P. Sokoloff, F.B. Colstoun, S.G. Lee, R. Jin, E.M. Wright, G. Khitrova, H.M. Gibbs, S.W. Koch, and N. Peyghambarian, *Phys. Rev. Lett.* **69**, 852 (1992).
- [9] P.F. Liao and G.C. Bjorklund, *Phys. Rev. B* **15**, 2009 (1977).
- [10] S.T. Ho, C.E. Socolich, M.N. Islam, W.S. Hobson, A.F.J. Levi, and R.E. Slusher, *Appl. Phys. Lett.* **59**, 2558 (1991).
- [11] M.N. Islam, C.E. Socolich, R.E. Slusher, A.F.J. Levi, W.S. Hobson, and M.G. Young, *J. Appl. Phys.* **71**, 1927 (1992).
- [12] G.M. Gale and A. Mysyrowicz, *Phys. Rev. Lett.* **32**, 727 (1974).
- [13] N. Nagasawa, N. Nakata, Y. Doi, and M. Ueta, *J. Phys. Soc. Jpn.* **39**, 987 (1975).
- [14] R. Levy, B. Hönerlage, and J.B. Grun, *Phys. Rev. B* **19**, 2326 (1979).
- [15] E. Hanamura, *J. Phys. Soc. Jpn.* **39**, 1516 (1975).
- [16] R. Levy, B. Hönerlage, and J.B. Grun, in *Optical Nonlinearities and Instabilities in Semiconductors*, edited by H. Haug (Academic Press, Boston, 1988).
- [17] B. Hönerlage and F. Tomasini, *Solid State Commun.* **59**, 307 (1986).
- [18] P.N. Butcher and D. Cotter, *The Elements of Nonlinear Optics* (Cambridge University Press, Cambridge, 1990).
- [19] In  $\chi^{(3)}$ , we also neglect the term which has the factor of  $1/(\Omega_m - \Omega_T - \omega - i\gamma_m T)$ . This additional term is canceled by further terms. See, S. Schmitt-Rink and H. Haug, *Phys. Status Solidi* **113**, K143 (1982).
- [20] M. Kuwata, *J. Phys. Soc. Jpn.* **53**, 4456 (1984).
- [21] H. Akiyama, T. Kuga, M. Matsuoka, and M. Kuwata-Gonokami, *Phys. Rev. B* **42**, 5621 (1990).
- [22] T. Ikehara and T. Ito, *Solid State Commun.* **79**, 755 (1991).
- [23] R. Leonelli, A. Manar, J.B. Grun, and B. Hönerlage, *Phys. Rev. B* **45**, 4141 (1992).
- [24] T. Ito and T. Suzuki, *J. Phys. Soc. Jpn.* **45**, 939 (1978).
- [25] R. März, S. Schmitt-Rink, and H. Haug, *Z. Phys. B* **40**, 9 (1980).
- [26] H. Haug, R. März, and S. Schmitt-Rink, *Phys. Lett.* **77**, 287 (1980).
- [27] M. Kuwata and N. Nagasawa, *J. Lumin.* **31&32**, 867 (1984).